

# The bedrock river profile fitting and the indicative significance: a case study in Gyirong watershed of the Middle Himalaya

Lu Chen<sup>1</sup> and Qinghong Ran<sup>1,\*</sup>

<sup>1</sup> Institute of Humanity Resources in Western China, Chengdu Normal University,  
Chengdu, Sichuan, China

\*Corresponding author e-mail: 452947916@qq.com

**Abstract.** Area-slope (AS) Model focuses on quantitative study of bedrock river which has been widely used in the longitudinal profile simulation of bedrock and alluvial rivers, but many applications have failed to carefully consider the mechanism, fitting effect and applicability, resulting in unsatisfactory simulation results. In order to verify the channel profile analysis capability, the study analyzes the theoretical basis of AS model and applies to the river channel fitting and knickpoint identification in the Gyirong Watershed in the middle Himalayan Orogen. The results show that, for rivers with different equilibrium status, the fitting curves have different splattering patterns. More than 80% knickpoints locate on the elevation between 4000 –5050 m where coincided with Tibetan Himalayan Unit. Although climate affects the spatial distribution of knickpoints, the structure of Gyirong watershed have developed before modern climate pattern.

**Keywords:** bedrock river; Area-slope model; knickpoint; Gyirong Watershed; middle Himalaya.

## 1. Introduction

A bedrock river is a rock bound reach in the riverbank or riverbed [1]. On a time scale of 10 to 100 years, the river bed is intermittently covered with a thin layer of sediments, and the long-term material transport flux is greater than the sediment flux[2]. And on the hundreds of thousands of years or longer, either the channel segment or the overall river bed and riverbank are significantly eroded [3]. Numerous studies prove that bedrock rivers generally develop in passive continental margins [4], active collision zones [5, 6] and intracontinental tectonic zones[7]. The establishment of function relation in bedrock river physical properties since 1950s promotes quantitative study of river geomorphology [8, 9, 10]. The area-slope model (AS) has become the highlight of the bedrock river stream-power erosion models during the past decades. The theoretical basis of the model is the physical water and sediment processes generate kinetic energy and dominate the process of river evolution accompanied by the shearstress of the river[11,12], which could be described by the power function of the drainage area and the river gradient[13,14]. Nevertheless, the premise of AS model is a river in equilibrium which is unrealistically ideal. To be a mountain bedrock river erosion and uplift are generally inconsistent in time and space. Furthermore the scatter plots of the river profile are usually unexplained. Our research detailed the theoretical basis of AS model, discussed the methods of river profile fitting and knickpoint extraction based on Gyirong Watershed in the middle Himalayan Orogen in Tibet, China. We selected 6 fully developed sub-basins, compared the results of the fitting profiles and identified the river knickpoints. Finally, we analyzed the relationship between the profiles parameters, spatial distribution characteristics of the knickpoints with the topography, geological construction and climate. It could provide some insight to understand and apply the model.

## 2. Materials and methods

### 2.1 Study area

The Gyirong Watershed is 2,108.59 km<sup>2</sup>, 85°10′–85°40′E, 28°15′–28°45′N, lies on the border between Tibet China and central Nepal. It belongs to the Ganges River basin and the Mount Shishapangma near to its east side. The rivers in the northern part of the watershed are relatively

gentle, to the middle reaches the rate of decline increases until narrow and deep in the downstream and the riverbed and bank are strongly scoured (Fig.1).

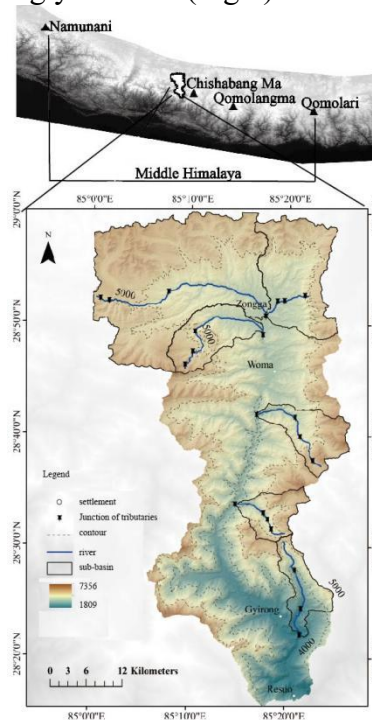


Figure 1. Topography of Gyirong Watershed

## 2.2 Data sources

ASTER GDEM and SRTM are two kinds of popular digital elevation models, but attention is rarely paid to the suitability of their data applications. The former is derived from the Terra satellite optical sensor while the latter from the STS Endeavour OV-105 radar carrier. Some people considered the latter to be more reliable in terms of rejecting the interference from surface cover [15]. In fact both datas have varying elevation differences of about 5.42m-5.31m in forest and city areas such as Central China and the Changbai Mountains [16,17]. They also could be used to evaluate the natural response of surface cover to terrain variations as well. For the Himalayan Mountains with dramatic differences in height, both of these datasets can display significant vertical zonality of the orogen and enhanced terrain features.

This paper adopted ASTER GDEM 2(<http://www.gscloud.cn>), because it has added 260,000-scene imagings and adopted correlation kernel calculations over a smaller space (5×5) (9×9 for GDEM 1) to solve the -5m overall skewness and water body shading problems of GDEM 1. It used multi-source data to fill in elevation voids and increased spatial resolution accuracy by one arc second (about 30m) (three arc seconds, or about 90m, for SRTM3 V2). This paper collected one ASTGTM file of the Gyirong River watershed [18], projected onto a UTM map at 45°N in ArcGIS 10.2. A vector geographic element data and 1:250000 geological map of Gyirong County were also selected, projected as same as the ASTGTM file.

## 2.3 Methods

### 2.3.1 Area-slope model

the classic expression of the AS model is rewritten as

$$S = k_s A^{-\theta} \tag{1}$$

where  $k_s$  is the river steepness index, and  $\theta$  is the concave index affecting the fluctuation of the river channels [10]. The assumption of the model is that if all of the water channels are in the same state, the discharge and the upstream drainage area have a power relationship. In fact the channels are formed by the interaction between the erosion process, the sediment flux of the riverbed and the resistance of the rock in the river and bank. Erosion rate can quantify the extent of the interaction. Accordingly, the shear stress against to the riverbed and bank is the process of erosion. Due to the degree of shear stress incision ranges from slight linear incision to strong abrasion [19], three variables, the discharge, the gradient and the channel width, are used in hydrology to describe the effects of shear stress on the riverbed. On the meanwhile, there is a power relationship between the discharge and the upstream drainage area and the channel width takes the form follow combined with the discharge. Finally equation (1) is obtained by the function relation between erosion rate and shear stress [10, 14]. It is usually written as

$$\ln S = \ln k_s - \theta \ln A \tag{2}$$

### 2.3.2 The river profiles fittings and knickpoints identification

The sub-watersheds selection. Firstly, we used the hydrologic analysis of ArcGIS 10.6 to calculate the river network and segment the sub-watersheds. The confluence of headwater determined by the threshold of flow acceleration is 1000 pixels, about 1 km<sup>2</sup> [20]. Strahler's river net gradient is adapted to recognize the river levels [21]. There are 74 sub-watersheds in Gyirong Watershed contained 5 levels in the river net even only 6 sub-watersheds have 4 levels of tributaries (Fig. 1).

River profile fitting. To extracted the 6 river masks onto Aster GDEM through the hydrologic analysis of ArcGIS. Then to smooth the 6 longitudinal profiles by least squares method with 10m interval sampling elevation [22]. We calculated the gradient and upstream drainage area based on the equation (1).

Knickpoints identify. An ideal isostatic channel pattern has three types of cknickpoint (Fig. 2(a)). Due to uplift and erosion, the river profile morphology in the upper and lower reaches of the cknickpoint usually changes abruptly. The logarithmic transformation of the smooth-fitting channel, as shown in Formula 2 (b), can show the crack location or potential crack points.

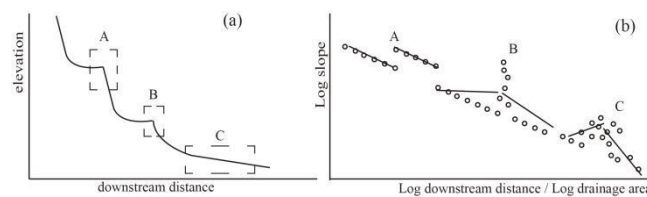


Figure 2 diagram of an ideal river profile and three kinds of cknickpoint.

- (a) an ideal equilibrium river profile;
- (b) the logarithmic transformation of the fitting channel.

## 3. Results

### 3.1 river fitting features of 4 classifications

By using AS model the fitting curves of six rivers were calculated (figure 3). From the area and gradient distributions of these smoothed rivers, the most equilibrium is river 1, followed by river 4. The most significant aggregation is river 2, followed by river 3 and 5. The characteristics of river 6 have both features of equilibrium and aggregation. It is relatively balanced on the first and second channels, and clustered on the third and fourth channels.

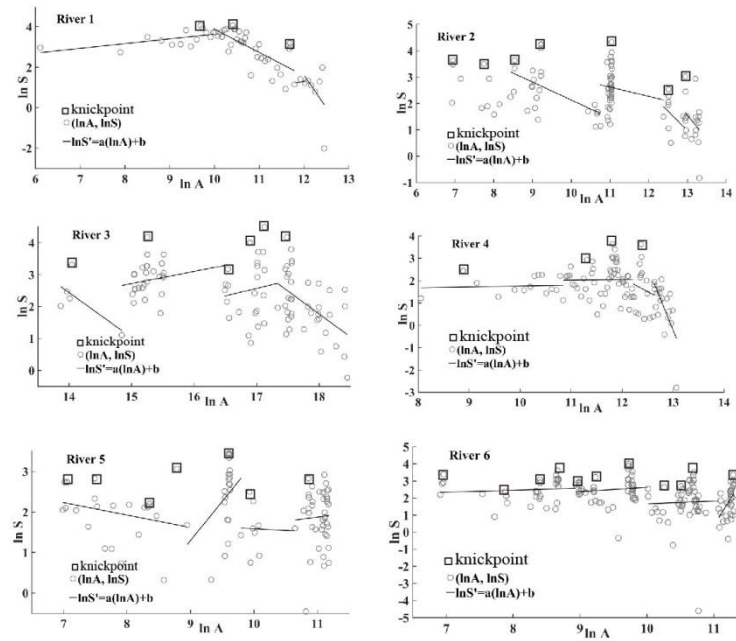


Figure 3 Fitting of river 1-6 profiles used equations 2.  $\ln S'$  is the fitting value.  $a$  and  $b$  are the regression coefficients. We invert  $a$  and  $b$  to get  $\theta$  and  $k_s$ .

### 3.2 Knickpoints

According to the identification characteristics of knickpoint in Figure 2, 38 knickpoints were visually interpreted on the scatter plots of 6 river profiles, that is, 38 channel mutation locations. As shown in Figure 3, rivers 1 and 4 have the least number of cracks, with 3 and 4 respectively. The number of split points in rivers 2, 3 and 5 is in the middle, with 7, 6 and 7 respectively. There were 11 cracks in river 6, accounting for 29% of the total. The results of the three river types reflected by the number of split points are very similar to the results of channel fitting.

As shown in the figure 4, three of the 38 have elevations higher than 5050 m (located on Rivers 3 and 4). Only 4 knickpoints are below 4000m (located on River 5 and 6). Other 31 knickpoints have elevations between 4000 – 5050 m. the proportion is as high as 81%. With a gradient lower than  $25^\circ$  as the critical value of a stable hillside[23], we divided these knickpoints into the following 3 classifications: stable (gradient less than  $25^\circ$ ), unstable (gradient greater than  $25^\circ$  but less than  $75^\circ$ ), and extremely unstable (gradient higher than  $75^\circ$ ). Ten of the knickpoints were stable, 16 were unstable, and 5 were extremely unstable. Especially between 4000-5050m, there are 16 knickpoints, accounting for 68% of the total, with gradient greater than  $25^\circ$ , which belongs to the unstable.

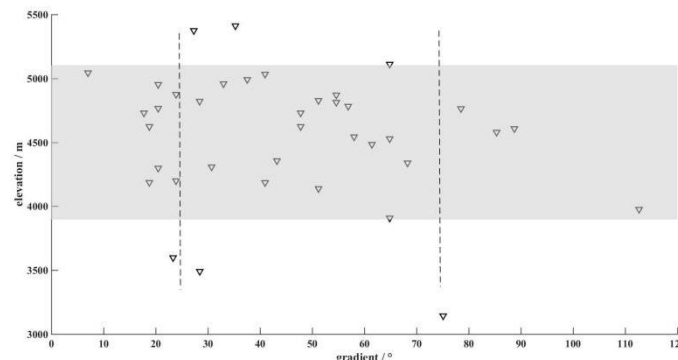


Figure 4 the slope and the elevation of 38 knickpoints.

The gray strip covers the interval elevation from 3950m to 5050m.  
 The two dotted lines point to 25° and 75° of slope.

## 4. Discussion

### 4.1 Comparison of AS Model Parameters

This study applies the AS model to simulate the form and structure of the river and to indicate the potential location of the knickpoints. To reduce the fitting error, we applied regression analysis based on equation 6 to the river network classifications and fit each river according to four regression equations (Fig.4). Then invert the  $\theta$  and  $k_s$  from equation 6 as well (table 1). In order to compare the fitting effect of AS model on different rivers, the error standard (ES in table 1) between the fitting gradient value  $\ln S'$  and the smoothed gradient value  $\ln S$  is further calculated. The smaller the ES value, the more concentrated the error between the fitted gradient and the actual gradient became, and thus, the better the model's fitting performance became. River 1 and River 2 have the best fitting effects, and both of ES are  $< 1$ . From the values of steepness index  $k_s$  and the concave index  $\theta$  on the 4 tributaries of the two rivers are basically the same. It can be seen that both of the topography, lithology and structural characteristics should belong to the same type, so the river development process should be consistent. The values of ES of rivers 3, 4 and 5 are at the same level, about 1.5. The steepness indices of the three rivers are very different, and the convexity indices have no obvious rule. May suggest different surface and subsurface structural features ongoing. The ES of River 6 is greater than 2.6, indicating that the fitting channel of AS model in this basin is not as accurate as that of other rivers. However, according to the parameters of the regression, the  $\theta$  are all negative, and  $k_s$  positive and  $< 5$ . Compared with the other 5 rivers, this river is the most equilibrated.

Table 1 the fitting parameters and fitting errors of the 6 river profiles

	first		second		third		forth		ES
	$\theta$	$k_s$	$\theta$	$k_s$	$\theta$	$k_s$	$\theta$	$k_s$	
River 1	0.263 1	22.4262	-0.8960	0.000 0	0.0941	8.4761	1.0431	1.7029E+ 06	0.493 3
River 2	0.263 1	22.4262	-0.8960	0.000 0	0.0941	8.4761	1.0431	1.7029E+ 06	0.726 9
River 3	1.237 2	1.5042E+ 08	-0.4237	0.012 6	0.6495	0.0001	1.9933	8.4308E+ 15	1.681 1
River 4	-0.03 94	3.9085	-0.0211	5.993 6	1.2244	1.9968E+0 7	5.6294	4.9035E+ 31	1.572 4
River 5	0.306 9	79.7671	-1.9389	0.000 0	0.0800	10.8000	-0.202 0	0.7048	1.653 4
River 6	-0.11 97	4.4515	-0.2429	1.203 7	-0.158 3	1.0727	-6.254 9	0.0000	2.641 6

### 4.2 Response of River Distribution Characteristics to Topography and Structure

It has been calculated that there are 74 sub-basins in the Gyrong Watershed, but only 6 have grade 4 tributaries. From the perspective of elevation, the sub-basins of rivers 1 to 5 are all located at 4000m-5000m, coincided with the Tibetan Himalayan unit. the river 6 sub-basin spans a large elevation interval, from 2300m to 4900m, traversing the higher Himalaya and the Tibetan Himalaya including the Southern Tibet Detachment Structure (STDS) unit. However, from the regression parameters fitted by AS model, the  $\theta$  of most tributaries is between  $\pm 2$ , which is not abnormally dispersed. Only the fourth tributaries of River 1 and 6 have values of more than  $\pm 5$ .

Field survey shows that the fourth tributaries of the fourth rivers have a large drop gap with the main stream, Gyirong Zangpo. This section is located at the topographic transformed elevation of 4000m and enters the STDS of intense fault movement.

The geological substrata in the interval of elevation 4000-5600m are the Tethys-Himalaya sedimentary fold-and-thrust belt. The famous wide alluvial valley Gyirong Basin is located here. The area of the 5 sub-watersheds of rivers 1 to 5 contained accounts for 68% in the elevation interval. The hanging wall of the Boerjilajia-Qionggga reverse fault is composed of Jurassic-Cretaceous shallow marine clastic, carbonatite, and siliceous rocks sedimentary formations, while the footwall consists of Sinian-Jurassic marine clastic and carbonatite [24,25]. It can be seen that the climate and lithology of this area have homogeneity. The secondary and the third tributaries of river 1 to 5 seem to reflect this heterogeneity, and their convexity values are basically the same. Researchers have pointed out that three elevation intervals of 2000-2200m, 2800-3000m and 4000m-5600m had a mean slope of  $25^\circ$  with consistently steady variability in local relief [26]. Only river 6 flows through the three elevations. From the values of  $\theta$  and  $k_s$  in table 1, there is no obvious mutation value of river 6, indicating that the development time is the longest among the six rivers.

### 4.3 Response of knickpoints spatial distribution to topography, structure and climate

The knickpoints exhibit significant spatial variation, and their classification is strongly influenced by their structural intensity. The stable knickpoints are concentrated in the Tibetan Himalayas, which have less relief. 10 stable knickpoints on rivers 1 - 3 account for 4/5 of the total number of stable knickpoints. In contrast, the unstable knickpoints are densely distributed at the intersections of rivers and in major faults and folds where tectonic deformation is quite intense, e.g., the upper plate of the Eastern Oma normal fault (R1a, R1b) and the axis of the Gongdang-Gunda anticline (R4a, R4c). In particular, there are 16 unstable knickpoints on rivers 5 - 6 on the lower plate of the Langgele normal fault. In addition, the extremely unstable knickpoints are concentrated in the area where the Shale reverse faults.

It has been reported that climate also affects the spatial distribution of knickpoints. In particular, knickpoints are often found in areas of retrogressive erosion in rivers with abundant rainfall and strong surface runoff [15, 27-28]. To some extent, the knickpoints identified in this study are related to the modern climate of the Gyirong Watershed. The stable knickpoints are primarily located at elevations of more than 4000 m where the annual precipitation is less than 300 mm [29] and seasonal glacial meltwater and weathering are the main causes of erosion. A large number of extremely unstable knickpoints are located in the Gyirong Valley where the annual precipitation is greater than 1000 mm [29], the terrain undulates significantly, and erosion is significantly stronger than at an elevation of 4000 m. However, the distribution of the knickpoints is not necessarily determined by the different climate patterns. As a matter of fact, the geomorphology at elevations of 2000 m to 7000 m in the Gyirong Watershed did not develop until the Late Pleistocene. The climatic differences are determined by the timing of the uplift and the corresponding elevation change in the mountain.

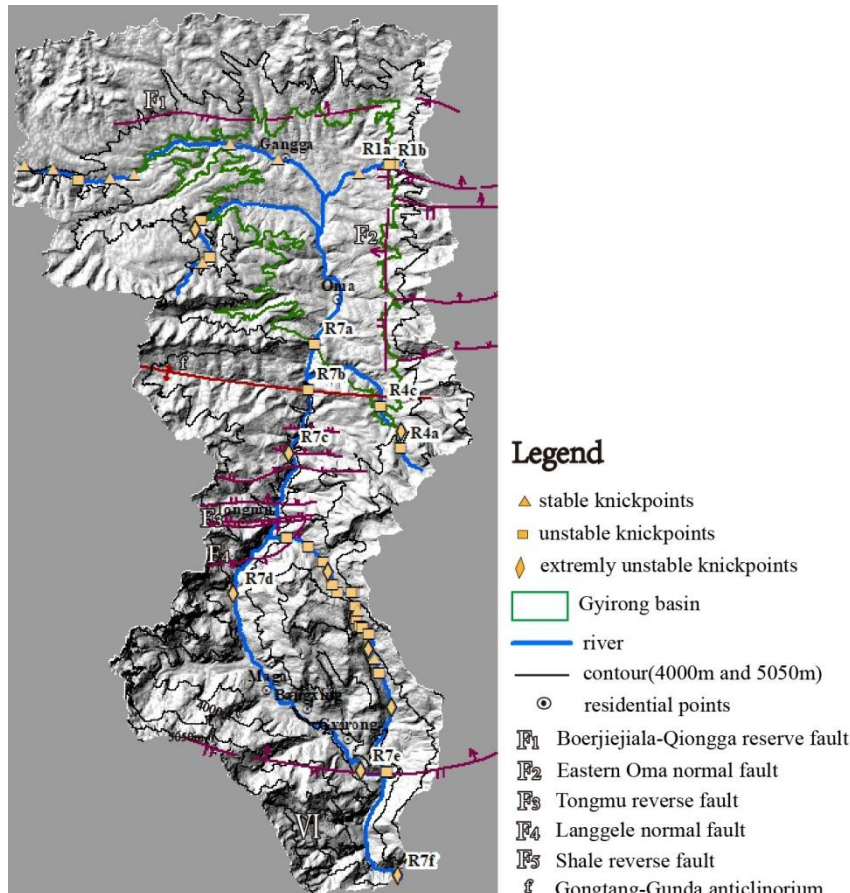


Figure 5 The relationship between tectonic, terrain and spatial distribution of the knickpoints

## 5. Conclusions

The double logarithmic scatter plots of area and slope for rivers with different equilibrium states can better reflect the information of knickpoints. But we must pay attention to the selection of smooth distance which must be suitable for applied DEM. Otherwise, the sensitive sections of river gradient changes are easy to be smoothed and lose some information. The AS model have different numerical responses to rivers with different levels of equilibrium. River 1 and River 2 have the best fitting effects, and both of fitting standard errors are  $< 1$ . The two rivers locate at the north of Gyrong watershed, deeply in the broad flat tectonic basins of Tibetan Himalaya. It can be seen that the two rivers belong to the same type with consistent development process. River 3, 4 and 5 have larger values of fitting standard errors, that may suggest the three sub-basins have more intensive activity ongoing. There are 5 rivers developed at the elevation above about 4000m, resulting in 31 (81% of the total account) knickpoints distributed at 4000-5000m. Among them, 10 stable knickpoints on rivers 1 - 3, 16 unstable knickpoints on rivers 5 - 6.

The spatial distribution of rivers and knickpoints is strongly constrained by terrain and structure. The rivers 1 to 5 are all located at 4000m-5000m, coincided with the Tibetan Himalayan unit. The stable knickpoints are concentrated in the Tibetan Himalayas as well, which have less relief. The river 6 spans from 2300m to 4900m, traversing the higher Himalaya and the Tibetan Himalaya including the STDS zone. And the 16 unstable knickpoints on rivers 5 - 6 on the lower plate of the Langele normal fault. Although the climate affects the spatial distribution of knickpoints by erosive process, the stable  $\theta$  and  $k_s$  of River 6 in the area of intense tectonic activity shows the structure of Gyrong watershed have developed before modern climate pattern.

## Acknowledgments

This research was funded by The Project of Talent Introduction by Chengdu Normal University grant number YJRC2016-6, and Scientific Research Project, grant number CS22XMPY0115. Thanks to the research materials from The University Demonstration Major on Curriculum Ideological and Political Education of the Higher education in Sichuan Province - Geographica Science (2022SJKCSZ01).

## References

- [1] Whipple, K.X.; DiBiase, R.A.; Crosby, B.T. *Bedrock Rivers*. In *Treatise on Geomorphology*; Shroder J., Wohl E.; Publisher: Academic Press, San Diego, CA, 2013; *Fluvial Geomorphology*, pp. 550-573.
- [2] Howard, A.D. Long profile development of bedrock channels: interaction of weathering, mass wasting, bed erosion, and sediment transport. In *Rivers over Rock: Fluvial processes in bedrock channels, geophysical sonograph series*; Tinkler K.; Wohl E.E. Publisher: AGU Press, Washington D C, 1998, pp. 297-319.
- [3] Montgomery, D.R. et al. Distribution of bedrock and alluvial channels in forested mountain drainage basins. *Nature*. 1996, 381, pp. 587-589.
- [4] Bishop, P. & Goldrick, G., 2000. Geomorphological evolution of the East Australian continental margin. In: S.M. A (S.M. A), *Geomorphology and Global Tectonics*. Wiley, Chichester, pp. 227-255.
- [5] Brookfield, M.E., 2008. Evolution of the great river systems of southern Asia during the Cenozoic India-Asia collision: Rivers draining north from the Pamir syntaxis. *Geomorphology* 100(3-4), 296-311..
- [6] Kirby, E., Whipple, K.X., Tang, W. & Chen, Z., 2003. Distribution of active rock uplift along the eastern margin of the Tibetan Plateau: inferences from bedrock channel longitudinal long profiles. *Journal of Geophysical research* 108, 2217.
- [7] Formento-Trigilio, M.L. & Pazzaglia, F.J., 1998. Tectonic geomorphology of the Sierra Nacimiento: traditional and new techniques in assessing long-term landscape evolution in the southern Rocky Mountains. *Journal of Geology* (106), 433-453.
- [8] Hack, J.T., 1957. *Studies of Longitudinal Stream Profiles in Virginia and Maryland*. Geological Survey Professional Paper 294, 45-97.
- [9] Flint, J.J., 1973. Stream gradient as a function of order, magnitude, and discharge. *Water Resources Research* 10(5), 969-973
- [10] Howard, A.D., Dietrich, W.E. & Seidl, M.A., 1994. Modeling fluvial erosion on regional to continental scales. *Journal of Geophysical Research-Solid Earth* 99(B7), 13971-13986
- [11] Dong, S.P., Zhang, P.Z., Zhang, H.P., Zheng, W.J. and Chen, H.X.. Drainage Responses to the Activity of the Langshan Range-Front Fault and tectonic implication. *Journal of Earth Science*, 2018, 29(1): 193-209
- [12] Perron, J.T. and Royden, L. An integral approach to bedrock river profile analysis. *Earth Surface Processes and Landforms*, 2013, 38(6): 570-576
- [13] Willgoose, G., 1994. A physical explanation for an observed area-slope-elevation relationship for catchments with declining relief. *Water Resources Research* 30(2), 151-159
- [14] Howard, A.D. & Kerby, G., 1983. Channel changes in badlands. *Geological Society of America Bulletin* 94(6), 739-752
- [15] Gong-Saholiariliva, N., Gunnell, Y., Harbor, D. & Mering, C., 2011. An automated method for producing synoptic regional maps of river gradient variation: Procedure, accuracy tests, and comparison with other knickpoint mapping methods. *Geomorphology* 134(3-4), 394-407
- [16] Zhao Guo Song, Du Yun, Lin Feng et al. Analysis of Influencing Factors on Height Differences between ASTER GDEM and SRTM3. *Science of Surveying and Mapping*, 2012, 37(4):167-170.(in Chinese)

- [17] Guo Xiao Yi, Zhang Hong Yan, Zhang Zheng Xiang et al. Comparative Analysis of the Quality and Accuracy between ASTER-GDEM and SRTM3. *Remote Sensing Technology and Application*, 2011, 26(3):334 - 339. (in Chinese)
- [18] USGS, Earth Remote Sensing Data Center. ASTER GDEM 2 README.2011. <https://lpdaac.usgs.gov>
- [19] Anderson, R., Hancock, G. & Whipple, K., 2015. River incision into bedrock: Mechanics and relative efficacy of plucking, abrasion, and cavitation. *Geological Society of America Bulletin* 112(3), 490-503
- [20] Montgomery, D.R. & Foufoula-Georgiou, E., 1993. Channel Network Source Representation Using Digital Elevation Models. *Water Resources Research* 29(12), 3925-3934
- [21] Strahler, A.N., 1953. Hypsometric (area-altitude) analysis of erosional topography. *Geological Society of America Bulletin* 63(11), 1117-1142
- [22] Snyder, N.P., Whipple, K.X., Tucker, G.E. & Merritts, D.J., 2000. Landscape response to tectonic forcing: Digital elevation model analysis of stream profiles in the Mendocino triple junction region, northern California. *Geological Society of America Bulletin* 112(8), 1250-1263
- [23] Kühni, A. & Pfiffner, O.A., 2001. The relief of the Swiss Alps and adjacent areas and its relation to lithology and structure: topographic analysis from a 250-m DEM. *Geomorphology* 41(4), 285 - 307.
- [24] Zhang, Z.L., 2003. Regional geological survey report of Gyirong of the People's Republic of China. China Geological Survey
- [25] Struth, L., Garcia-Castellanos, D., Viaplana-Muzas, M. & Vergés, J., 2019. Drainage network dynamics and knickpoint evolution in the Ebro and Duero basins: From endorheism to exorheism. *Geomorphology* 327, 554-571
- [26] Chen Lu, Kan Aike, Wang Yingjie. The small-scale Tectonic Landforms of Gyirong Watershed in the Middle Himalayan Orogen, Tibet, China. *Garpathian Journal of Earth and Environmental Sciences*, 2019, 14(2): 473-482
- [27] Ahmed, M.F., Rogers, J.D. & Ismail, E.H., 2018. Knickpoints along the upper Indus River, Pakistan: an exploratory survey of geomorphic processes. *Swiss Journal of Geosciences* 111(1-2), 191-204
- [28] Zhang, Z.L., Sun, X., Li, G.D, Zhang J.D., Liu H.Z., Zhuan S.P. & Wei W.T., 2006. New explanation of detachment structures in the Burang and Gyironggou regions, southern Xizang. *Sedimentary Geology and Tethyan Geology* 26(2), 1-6
- [29] Yang, R.F., 2011. Study on the Chongzhui accumulation body's cause of formation of Gyirong Basin. Chengdu University of Technology. pp.11